

# Nucleolar protein CSIG is required for p33ING1 function in UV-induced apoptosis

N Li<sup>1</sup>, G Zhao<sup>1</sup>, T Chen<sup>1</sup>, L Xue<sup>1</sup>, L Ma<sup>1</sup>, J Niu<sup>1</sup> and T Tong<sup>\*,1</sup>

**Cellular senescence-inhibited gene (CSIG) protein, a nucleolar protein with a ribosomal L1 domain in its N-terminus, can exert non-ribosomal functions to regulate biological processes, such as cellular senescence. Here, we describe a previously unknown function for CSIG: promotion of apoptosis in response to ultraviolet (UV) irradiation-induced CSIG upregulation. We identified p33ING1 as a binding partner that interacts with CSIG. After UV irradiation, p33ING1 increases its protein expression, translocates into the nucleolus and binds CSIG. p33ING1 requires its nucleolar targeting sequence region to interact with CSIG and enhance CSIG protein stability, which is essential for activation of downstream effectors, Bcl-2-associated X protein, to promote apoptosis. Thus, our data imply that p33ING1–CSIG axis functions as a novel pro-apoptotic regulator in response to DNA damage.**

*Cell Death and Disease* (2012) 3, e283; doi:10.1038/cddis.2012.22; published online 15 March 2012

**Subject Category:** Cancer

The nucleolus is the site for rRNA synthesis and ribosome assembly in the cell. Recent studies showed that the nucleolus has emerged as a highly complex and multi-functional regulatory compartment.<sup>1,2</sup> The nucleolus is an extremely sensitive structure to monitor; it responds to cellular apoptotic stresses such as radiation, or exposure to cytotoxic agents.<sup>3,4</sup> Nucleolar proteins such as nucleophosmin (NPM/B23), nucleostemin, L11, Net1 and ARF (alternate reading frame product of the CDKN2A locus) have important roles in these non-ribosomal functions, including regulation of cell growth and death, stress responses, mitosis and the cell cycle; we are only just beginning to understand.<sup>3,4</sup>

Cellular senescence-inhibited gene (CSIG) protein (RSL1D1/PBK1/L12) is a protein first cloned by several labs including ours. It is a nucleolar protein that has a ribosomal L1 domain in its N-terminus and a lysine-rich domain in its C-terminus.<sup>5</sup> This protein can delay cellular senescence through inhibition of phosphatase and tensin homolog protein (PTEN) translation.<sup>5</sup> It also can regulate the nucleolar localization of nucleostemin through physical interaction by its C-terminus.<sup>6</sup> Whether CSIG can modulate response to pro-apoptotic stimuli is currently unknown.

Protein complex shuttles between the nucleolus and nucleoplasm are important for many non-ribosomal processes.<sup>4,7</sup> Protein movement is mostly out of, rather than into, the nucleolus in response to DNA damage.<sup>8</sup> Few proteins seem to be targeted to the nucleoli after damage; the known examples include p33ING1, RelA, DEDD, heat-shock protein-70 (Hsp70) and PML, which migrate from the nucleoplasm or cytoplasm.<sup>9–13</sup> The p33ING1 tumor suppressor has been

reported to be downregulated in breast, gastric and lymphoid tumors.<sup>14</sup> p33ING1 promotes apoptosis, and its movement to the nucleolus increases apoptosis after ultraviolet (UV) irradiation.<sup>12,15,16</sup> p33ING1 possesses a nucleolar targeting sequence (NTS); mutation in this sequence was found to reduce p33ING1 apoptotic function after UV treatment.<sup>12</sup> ARF protein, which localizes predominantly in the nucleolus, physically associates with p33ING1 and causes cell-cycle arrest in the absence of UV stress.<sup>17</sup> However, ARF moves from the nucleolus to the nucleoplasm in response to UV – in a direction opposite to p33ING1 movement.<sup>18,19</sup> Why p33ING1 protein targets the nucleolus to promote apoptosis in response to UV has been unclear.

Here, we report that increased protein expression of CSIG sensitizes cells to UV irradiation-induced apoptosis. p33ING1 targets the nucleolus and stabilizes CSIG protein after UV irradiation. We show here that p33ING1 needs its NTSs to interact with CSIG, which is required for CSIG protein stabilization and p33ING1-dependent apoptosis after UV stress. Also, knocking down CSIG expression decreases p33ING1-dependent apoptosis after UV irradiation. Our results provide a new possible molecular mechanism underlying the regulation of apoptosis after UV irradiation.

## Results

**CSIG promotes UV irradiation-induced apoptosis.** Many nucleolar proteins respond to DNA damage.<sup>3</sup> To examine whether CSIG affects the ability of cells to undergo apoptosis in response to genotoxic stress, we initially analyzed CSIG

<sup>1</sup>Research Center on Aging, Department of Biochemistry and Molecular Biology, Peking University Health Science Center, 38 Xueyuan Road, Beijing 100191, People's Republic of China

\*Corresponding author: T Tong, Research Center on Aging, Department of Biochemistry and Molecular Biology, Peking University Health Science Center, 38 Xueyuan Road, Beijing 100191, People's Republic of China. Tel: +86 10 82802931; Fax: +86 10 82802931; E-mail: ttj@bjmu.edu.cn

**Keywords:** apoptosis; CSIG; p33ING1; Bax; nucleolar protein; UV irradiation

**Abbreviations:** CSIG, cellular senescence-inhibited gene protein; Bax, Bcl-2-associated X protein; PTEN, phosphatase and tensin homolog protein; ARF, alternate reading frame product of the CDKN2A locus; NLS, nuclear localization signal; NTS, nucleolar targeting sequence; HSP70, heat-shock protein-70; PARP, poly (ADP-ribose) polymerase; COX IV, cytochrome c oxidase IV; uPA, urokinase-type plasminogen activator; IP, immunoprecipitation; siRNA, small interfering RNA  
Received 05.9.11; revised 17.1.12; accepted 02.2.12; Edited by P Salomoni

expression levels after DNA damage. When HEK293 cells were treated with UV, etoposide, low and high concentrations of cisplatin and doxorubicin to induce genotoxic stress, the cells significantly upregulated CSIG after treatment (Figure 1a). To further investigate a possible role for CSIG in UV-induced apoptosis, we transfected HEK293 cells with a control vector or a plasmid expressing wild-type CSIG and subjected the cells to UV treatment (Figure 1b). Apoptosis was shown by Annexin-V and PI double staining; percentage of the sub-G1 fraction by FACS analysis; and chromatin condensation by 4,6-diamidino-2-phenylindole (DAPI) staining. The results showed that overexpression of CSIG did not induce apoptosis in the absence of DNA damage (Figure 1c). However, after UV treatment, CSIG increased the population of apoptotic cells (Figure 1d, Supplementary Figure S1b). Overexpression of CSIG also increased the population of apoptotic cells after doxorubicin treatment (Supplementary Figure S1). Cell-cycle profiles of the cells were also shown; overexpression of CSIG slightly decreased G<sub>1</sub>-phase percentage and increased S-phase and

G<sub>2</sub>/M-phase cell numbers, but there was no significant difference compared with controls, both in non-UV and UV treatment (Figures 1c and d).

**Ultraviolet irradiation can induce both CSIG and p33ING1 protein expressions.** We found that CSIG protein induction after UV is independent of p53 status (data not shown). So there may be other proteins participating in this process. p33ING1 is a putative tumor suppressor, which promotes apoptosis in a p53-dependent or -independent manner.<sup>15,20–23</sup> Ultraviolet irradiation targets p33ING1 to the nucleolus to promote apoptosis; CSIG primarily localizes in the nucleolus,<sup>5,12</sup> and CSIG increased UV-induced apoptosis (Figure 1). To determine if there is a functional relationship of CSIG with p33ING1 in UV-induced apoptosis, their cellular localizations and expression patterns were examined.

Subcellular distributions of CSIG and p33ING1 were determined by high-resolution confocal analyses. The results showed that CSIG protein localized predominantly in the

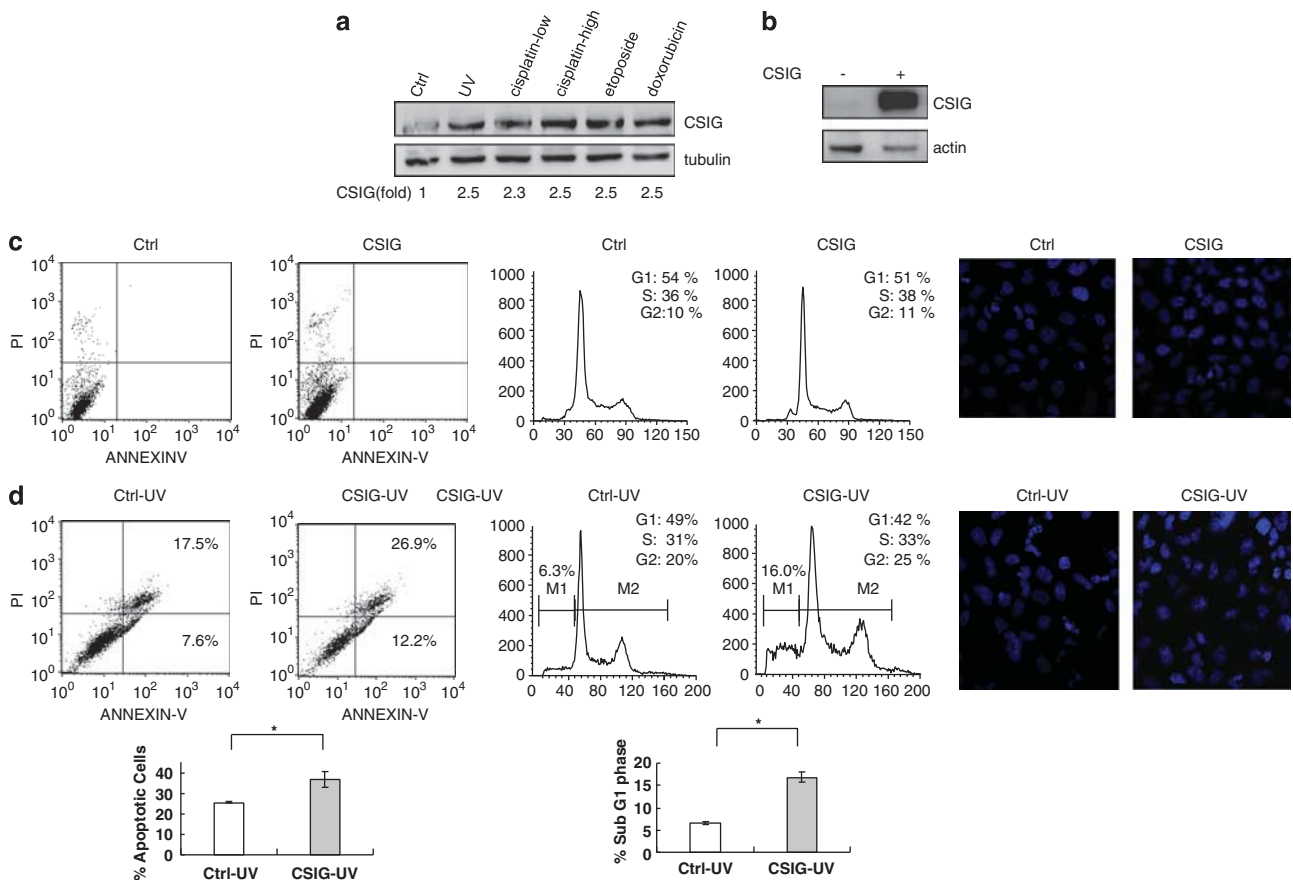


**Figure 1** CSIG sensitizes cells to UV-induced apoptosis. (a) HEK293 cells were treated with 50 J/m<sup>2</sup> UV, etoposide (50  $\mu$ M), and low (1  $\mu$ g/ml) and high (10  $\mu$ g/ml) concentrations of cisplatin and doxorubicin (2  $\mu$ M). After 6 h, cells were harvested for western blot analysis. Tubulin was used as loading control for western blot analysis. The relative abundance of CSIG was measured by densitometry and expressed as fold increase relative to control cells. (b) HEK293 cells were transfected with plasmids for CSIG or empty control vector. The cells were lysed and tested by western blotting for CSIG and  $\beta$ -actin expression. (c) HEK293 cells were transfected with plasmids for CSIG or empty control vector, and 48 h later were collected for apoptotic assays. (d) HEK293 cells were transfected with plasmids for CSIG or empty control vector, and 36 h later were irradiated with 50 J/m<sup>2</sup> UVC and cultured for 24 h. Floating and adherent cells were collected for apoptotic assays. For AnnexinV-FITC and PI analysis, cells stained by AnnexinV or both dyes were regarded as apoptotic. For cell-cycle analysis, cells were harvested, fixed and stained by PI. Horizontal bars mark areas quantified to determine the proportion of cells with the indicated DNA content. M1 indicate apoptotic cells with sub-G1 DNA content. Values are means  $\pm$  S.D. \* $P \leq 0.05$ . Chromatin condensation was visualized by DAPI staining and analyzed with immunofluorescence microscopy. The cells that were condensed, fragmented and bright were regarded as apoptotic cells

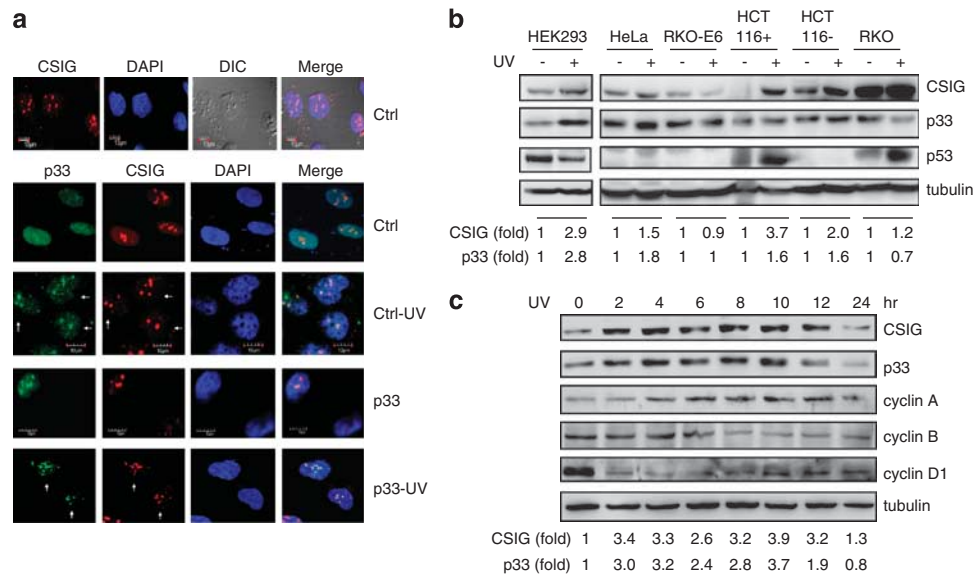


**Figure 2** The protein expression and colocalization of CSIG with p33ING1 after UV irradiation. (a) Representative images of cells stained for p33 (green) and CSIG (red) by indirect immunofluorescence. The localization of endogenous CSIG was immunostained with anti-CSIG antibody, followed by confocal microscopy analysis. The nucleoli were shown in differential interference contrast (DIC) images (upper panel). HEK293 cells were transfected with control vector or an expression vector for p33, left untreated or irradiated by UV; 6 h later, cells were immunostained with anti-p33 and anti-CSIG antibodies, followed by confocal microscopy analysis (lower panel). Representative images are shown. Nuclei were visualized by DAPI staining and images were overlaid (Merge). White arrows indicate localization of proteins after UV irradiation. (b) HEK293, HeLa, HCT116 p53<sup>+/+</sup>, HCT116 p53<sup>-/-</sup>, RKO and RKO-E6 cells were irradiated with 50 J/m<sup>2</sup> UV; 6 h later, cells were collected separately for western blot analysis of CSIG, p33, p53 and tubulin. (c) HEK293 cells were irradiated with 50 J/m<sup>2</sup> UV and cells were collected at different time points as indicated. Immunoblot analysis was carried out using anti-CSIG, anti-p33, anti-cyclin A, anti-cyclin B, anti-cyclin D1 and anti-tubulin antibodies

nucleolus (Figure 2a upper panel). Endogenous p33ING1 was mostly distributed in the nucleus without treatment and gathered within the nucleolus after UV irradiation. Ectopically expressed p33ING1 increased its distribution both in the nucleus and in the nucleolus without UV irradiation; after UV irradiation, the exogenous p33ING1 gathered within the nucleolus. To a great extent, CSIG colocalized with both endogenous and exogenous p33ING1 protein in the nucleolus after UV irradiation (Figure 2a lower panel). These data suggest a physiological connection between CSIG and p33ING1 after UV irradiation.

Previous studies reported that p33ING1 increases the protein expression after DNA damage in some cell lines.<sup>20,24</sup> Also, CSIG protein levels upregulate after DNA damage treatments (Figure 1). So, we analyzed whether UV irradiation could induce p33ING1 and CSIG protein expressions in cell lines with different p53 status. Results showed CSIG and p33ING1 to be simultaneously induced after UV irradiation in HEK293 (p53 deregulation), HeLa (p53 deficient), HCT116 p53<sup>+/+</sup> (p53 wild-type) and HCT116 p53<sup>-/-</sup> (p53 null), but not RKO (p53 wild-type) and RKO-E6 (p53 deficient), cells. These results indicated that UV induced CSIG and p33ING1 expressions, which were p53 independent (Figure 2b). In addition to UV irradiation, p33ING1 and CSIG were simultaneously induced by the DNA damage treatments, including high concentration of cisplatin, etoposide and doxorubicin (Supplementary Figure S2).

To further study the protein expression profile of CSIG and p33ING1 after UV irradiation, we analyzed CSIG and p33ING1 expressions at different time points after UV irradiation. The results indicated that the expression pattern of p33ING1 paralleled CSIG after UV irradiation (Figure 2c).

The CSIG and p33ING1 protein expressions were rapidly induced in as early as 2 h after UV irradiation, reached their peak at 8–10 h and declined 12 h later. To determine whether the same kinetics of CSIG and p33ING1 after UV treatment was due to cell-cycle arrest, expressions of cyclin A, cyclin B and cyclin D1, which indicated different cell-cycle phase, were also detected. The results showed that the induction of CSIG and p33ING1 levels after UV treatment was not consistent with any phase of cell-cycle progression (Figure 2c).

#### p33ING1 inhibits CSIG protein degradation after UV irradiation.

To directly determine the correlation of CSIG and p33ING1 upregulation after UV irradiation, HEK293 cells were transfected with CSIG or p33ING1 plasmids, and then subjected to UV irradiation. Protein levels of CSIG under the condition of p33ING1 overexpression were examined, and vice versa. Western blot analysis showed that p33ING1 induced endogenous CSIG expression, and the induction of CSIG remained for at least 24 h after UV radiation (Figure 3a, Supplementary Figure S3a), while CSIG overexpression was unable to increase p33ING1 levels after UV (Figure 3b). To examine whether CSIG protein induction by p33ING1 after UV irradiation was due to increased CSIG transcription, CSIG mRNA levels were probed. Under the same conditions as the p33ING1 transfection, in which CSIG protein was significantly induced, CSIG mRNA levels just slightly increased (data not shown), indicating that p33ING1 may affect CSIG protein levels through other mechanisms. To examine whether induction of CSIG by p33ING1 was due to increased CSIG protein stability, we treated cells with proteasome inhibitor MG-132; adding MG-132 led to increased CSIG protein levels (Figure 3c). Also, p33

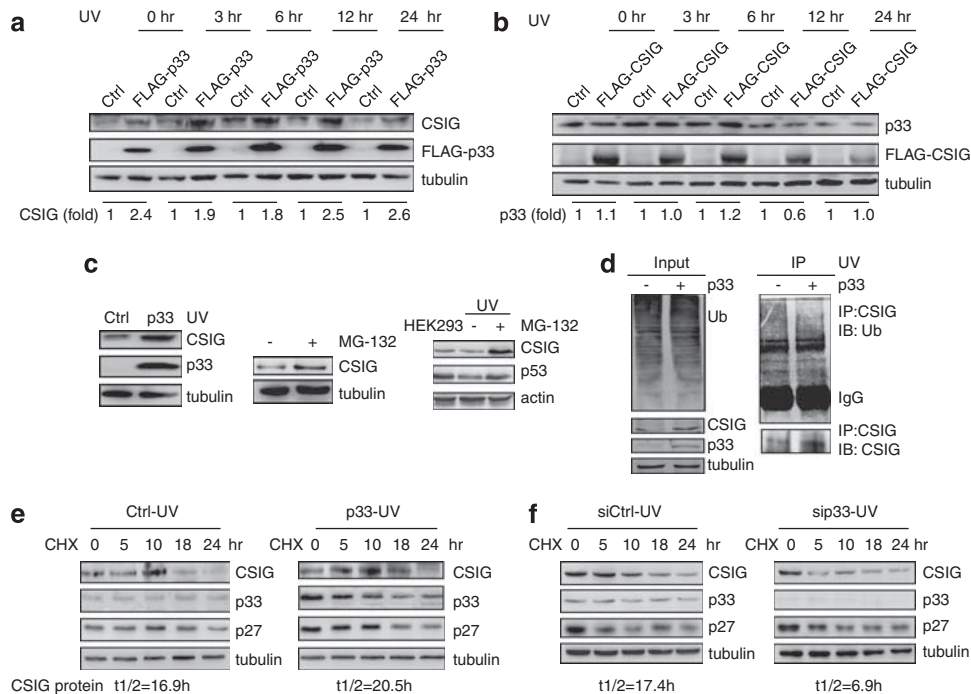


**Figure 3** p33ING1 overexpression increases CSIG protein stability after UV treatment. HEK293 cells were transfected with control vector or a vector expressing FLAG-tagged-p33 (a) or FLAG-tagged-CSIG (b); cells were then either left untreated or irradiated with 50 J/m<sup>2</sup> UV. Cells were harvested 3, 6, 12 and 24 h after irradiation, and western blots were performed to detect CSIG and p33 expressions. (c) HEK293 cells were transfected with control vector or a vector expressing p33; cells were then treated with UV. After 24 h, they were harvested for CSIG protein expression by western blot (left panel). HEK293 cells were non-treated (middle panel) or irradiated by UV at 50 J/m<sup>2</sup> and then recovered for 24 h (right panel). Cells were then treated with MG-132 (15 μM, 4 h), and CSIG levels were determined by western blotting. p53 was used as a positive control. (d) HEK293 cells were cotransfected with control or p33ING1 plasmid and HA-tagged ubiquitin plasmid; 36 h later, cells were irradiated with 50 J/m<sup>2</sup> UV. After 10 h, cells were treated with MG132 (15 μM) for 4 h. Cells were lysed and IP with CSIG antibody, then western blot using CSIG and ubiquitin antibodies. Also blot the input using ubiquitin, CSIG, p33 and tubulin antibodies. (e) pcDNA3.1 control vector or pcDNA3.1-p33 were transfected in HEK293 cells as indicated. At 36 h after transfection, cells were subjected to UV irradiation and treated with cycloheximide (CHX, 100 μg/ml) for the indicated times. CSIG protein levels were analyzed by western blotting. p27 levels were determined as positive control. (f) Control siRNA or specific siRNA against p33 were transfected in HEK293 cells as indicated. At 48 h after transfection, cells were subjected to UV irradiation and treated with CHX (100 μg/ml) for the indicated times. CSIG protein levels were analyzed by western blotting. p27 levels were determined as positive control. t1/2 of CSIG protein was calculated and listed below each group

increased CSIG protein by reducing its ubiquitination after UV irradiation (Figure 3d). We performed CSIG half-life assays in control and p33ING1-overexpression cells. After UV radiation, endogenous CSIG appeared to be unstable after 10 h of chasing in control cells (t1/2 = 16.9 h). However, in the presence of p33ING1 overexpression, CSIG protein became more stable and its protein level appeared to be unstable after 18 h of chasing (t1/2 = 20.5 h) (Figure 3e, Supplementary Figure S3b). We also examined the half-life of CSIG protein in control small interfering RNA (siRNA)- and p33ING1-specific siRNA-transfected cells after UV irradiation. Knocking down p33ING1 protein destabilized CSIG protein after UV treatment; endogenous CSIG appeared to be unstable after 5 h of chasing in p33 knockdown cells (Figure 3f).

**p33ING1 interacts with CSIG.** p33ING1 can stabilize p53 levels through interaction with it in different cell lines.<sup>25–27</sup> Having shown that p33ING1 increases CSIG protein stability and that they colocalized subcellularly in the nucleolus after UV irradiation, we investigated whether p33ING1 interacts with CSIG to stabilize its protein level.

*In vitro* pull-down assays using purified GST fusion proteins revealed a specific interaction between GST–CSIG and

*in vitro*-translated p33ING1, suggesting a direct CSIG–p33ING1 interaction (Figure 4a). The association between these two proteins *in vivo* was studied by immunoprecipitation (IP), followed by western blotting. Using total protein extracts from cells transfected with p33ING1 construct, a specific antibody against CSIG used in IP, we were able to detect both CSIG and p33ING1 in the immunocomplex. The interaction was specific, as shown by the use of a non-related serum. The association could also be observed in a reverse experiment, using the anti-p33ING1 IP antibody, indicating that the two proteins can associate in the cell (Figure 4b). Similar results were obtained using H1299 cells (data not shown). To confirm whether the observed interaction occurred between the endogenous proteins, we carried out IP experiments in untransfected 2BS cells. Using nuclear or cytoplasm protein extracts, a specific antibody against CSIG was used for IP. Western blotting revealed a specific band comigrating with p33ING1 in the CSIG immunoprecipitate of nuclear protein extracts, indicative of interaction between the endogenous p33ING1 and CSIG proteins in the nucleus. We did not detect another nucleolus protein, ARF, which reportedly mediates nucleolar localization of p33ING1 in the p33ING1/CSIG complex under these conditions (Figure 4c). After UV irradiation, the association between p33ING1 and CSIG

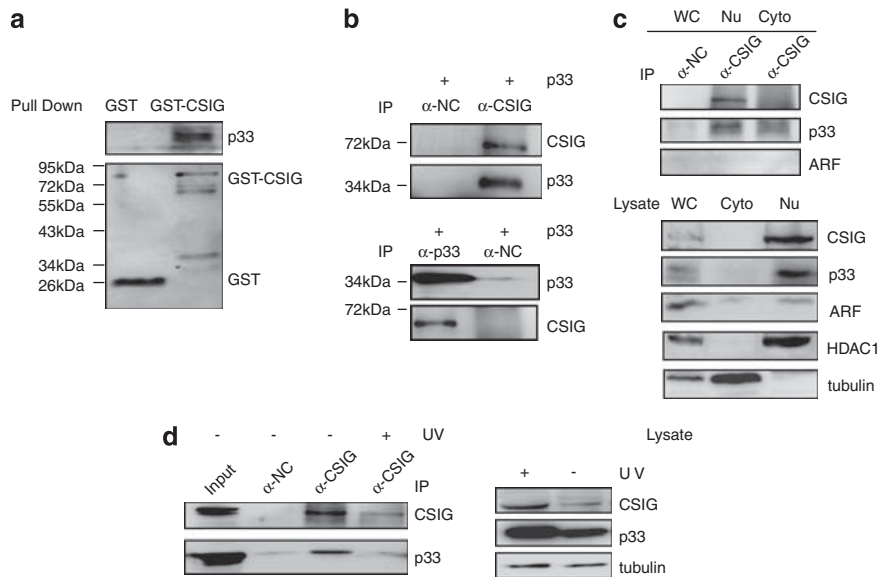


**Figure 4** p33ING1 interacts with CSIG. **(a)** CSIG was expressed as a GST fusion protein and incubated with *in vitro*-translated p33. GST or GST-CSIG proteins were precipitated with glutathione-Sepharose, and the coprecipitation of p33 was determined by western blotting with an anti-p33 antibody. **(b)** HEK293 cells were transfected with p33. At 48 h after transfection, whole-cell extracts were immunoprecipitated with an anti-CSIG (upper panel) or anti-p33 antibody (lower panel). Western blot analysis was performed with anti-CSIG and anti-p33 antibodies as indicated. **(c)** Nuclear or cytoplasmic extracts from 2BS cells were immunoprecipitated with an anti-CSIG antibody (upper panel). Cell lysates were loaded as a control (lower panel). Western blot analysis was performed with indicated antibodies. HDAC1 and  $\alpha$ -tubulin served to assess the quality the nuclear and cytoplasmic extracts. **(d)** Whole-cell extracts from HEK293 cells before and 6 h after UV irradiation (50 J/m<sup>2</sup>) were immunoprecipitated with an anti-CSIG antibody (left panel). Cell lysates were loaded as a control (right panel). Also, western blot analysis was performed with anti-CSIG and anti-p33 antibodies. The lysate loaded onto the gel was 5% of that used in the IPs, and non-related serum (NC) served as a negative control in these IP experiments

increased (Figure 4d). Together, the data indicate that CSIG interacts physically with p33ING1 *in vitro* and *in vivo*.

**The p33ING1 NTS region is required for binding and stabilizing the CSIG protein.** After establishing that p33ING1 and CSIG coexist in the same complex, we investigated which domains are involved in the p33ING1-CSIG interaction. We constructed deletion mutants of both proteins, expressed them in HEK293 cells and tested their binding using Co-IP. FLAG-tagged CSIG (amino acids 1–490), CSIG-NT (amino acids 1–275) or CSIG-CT (amino acids 261–490) was expressed in HEK293 cells and immunoprecipitated with anti-FLAG antibodies. Western blotting revealed that p33ING1 associates with FLAG-CSIG and FLAG-CSIG-CT. FLAG-tagged CSIG-NT did not associate significantly with p33ING1. The association could also be observed in a reverse experiment, using the anti-p33ING1 antibody for IP (Figure 5a). On the other hand, FLAG-tagged p33 (amino acids 1–279), p33-NT (amino acids 1–212) and p33-CT (amino acids 70–279) were expressed in HEK293 cells and immunoprecipitated with anti-FLAG antibodies. Western blotting revealed that both p33ING1 deletion mutants were able to interact with CSIG; the association could also be observed in a reverse experiment, using the anti-CSIG antibody for IP (Figure 5b). This interaction region of p33ING1 compassed the lamin interaction domain and nuclear localization signal (NLS).

Reportedly, p33ING1 possess two distinct four amino-acid sequences in its NTS within the NLS region, directing the protein to the nucleolus.<sup>12</sup> We have shown that CSIG and p33ING1 colocalized in the nucleolus (Figure 2a). To examine whether the NTS region of p33ING1 is necessary for binding

CSIG, we constructed point mutations or deletion mutant of the NTS regions in p33ING1 (Figure 6a), and then investigated their nucleolar localization and interaction with CSIG. As depicted in Figure 6b, the p33/Q153P, p33/Q153P/K185N/K186E and p33 $\Delta$ 142–194 mutants of the NTS region were impaired in their ability to target p33ING1 to the nucleolus. Through IP of CSIG from cells expressing wild-type p33, p33/Q153P, p33/Q153P/K185N/K186E and deletion mutant p33 $\Delta$ 142–194, we found that wild-type p33 coimmunoprecipitated to a larger extent with CSIG than did the two mutants p33/Q153P and p33/Q153P/K185N/K186E, and the deletion mutant of NTS region p33 $\Delta$ 142–194 completely abolished binding between p33ING1 and CSIG (Figure 6c). These results demonstrate that the nucleolus targeting domain of p33ING1 is essential for binding the CSIG protein C-terminus.

We next investigated whether p33ING1 needs this region to increase CSIG protein stability after UV irradiation. We found that wild-type p33ING1 increased CSIG protein stability after UV irradiation; this effect was abolished when the p33 $\Delta$ 142–194 deletion mutant was transfected (Figure 6d).

**p33ING1 requires CSIG protein to increase apoptosis after UV irradiation.** Bcl-2-associated X protein (Bax) and HSP70, which regulate apoptosis, have been identified as direct downstream targets of p33ING1.<sup>15,28,29</sup> We previously reported that CSIG could regulate PTEN protein translation.<sup>5</sup> To determine whether CSIG is required for p33ING1 function after UV irradiation, HEK293 cells were transfected with wild-type p33, p33/Q153, p33/Q153/K185N/K186E or deletion mutant p33 $\Delta$ 142–194, and the expression levels of CSIG and their target genes were examined after UV treatment. p33ING1 overexpression increased CSIG protein

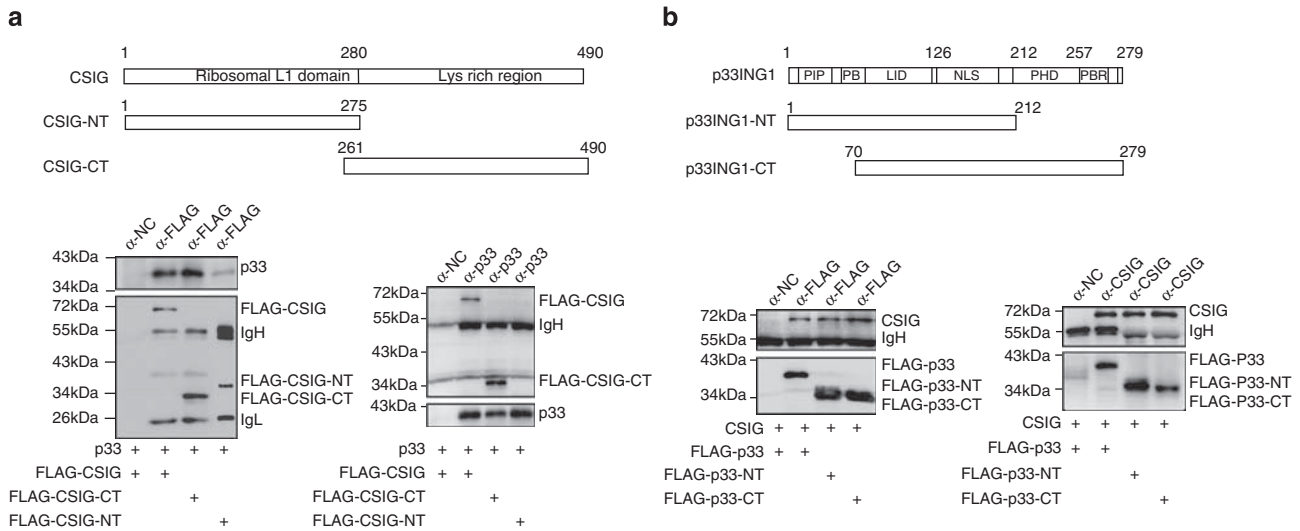


**Figure 5** p33ING1 interacts with the CSIG protein C-terminal lysine-rich region. (a) Schematic representation of CSIG deletion mutants, numbers indicate the position of amino acids in CSIG (upper). FLAG-tagged full-length and deletion mutants of CSIG were cotransfected with p33 plasmid in HEK293 cells. IP experiments were performed with anti-FLAG (left) or anti-p33 (right) antibody. Western blot analysis was performed with anti-FLAG and anti-p33 antibodies. (b) Schematic representation of p33 deletion mutants, numbers indicate the position of amino acids in p33 (upper). PIP, PCNA-interacting protein motif; PB, partial bromodomain; LID, lamin interaction domain; PHD, plant homeodomain; and PBR, polybasic region. FLAG-tagged full-length and deletion mutants of p33 were cotransfected with CSIG plasmid in HEK293 cells. IP experiments were performed with anti-FLAG (left) or anti-CSIG (right) antibody. Western blot analysis was performed with anti-FLAG and anti-CSIG antibodies

level and elevated its downstream target Bax expression after UV radiation, while HSP70 and PTEN expression did not greatly change. Compared with the effects of wild-type p33ING1, overexpression of CSIG-binding defective mutants p33/Q153, p33/Q153/K185N/K186E and particularly the deletion mutant p33 $\Delta$ 142–194 reduced the elevation of CSIG and Bax expressions, while HSP70 and PTEN expressions did not change much (Figure 7a). Similar results have been obtained using HeLa cells (Supplementary Figure S4a). Bax induced the release of apoptotic stimulators, such as cytochrome *c* to the cytoplasm, constituting a critical step in the mitochondrial apoptotic pathway. As wide-type p33, but not p33 $\Delta$ 142–194 mutant, induced CSIG and Bax expressions, we next determined the effects of p33 and p33 $\Delta$ 142–194 on Bax-dependent apoptosis in mitochondria after UV irradiation. The results showed that p33, but not the p33 $\Delta$ 142–194 mutant, induced Bax expression and distribution on the mitochondria, which coincides with the increased translocation of cytochrome *c* to the cytoplasm compared with control vector after UV treatment (Figure 7b). Consistent with these results, overexpression of p33ING1 enhanced UV-induced apoptosis, as shown by cleaved poly (ADP-ribose) polymerase (PARP), Annexin-V and PI double staining. Again, these effects were reduced by expression of p33ING1 mutants (Figures 7b and c). Thus, p33ING1 requires its NTS sequence to interact with CSIG, increase CSIG protein stability and activate target gene Bax after UV irradiation.

To directly determine whether p33ING1 requires CSIG protein to activate target gene and promote apoptosis after UV irradiation, HEK293 cells were transfected with vectors expressing p33ING1 and CSIG, or CSIG-specific siRNA, alone or in combination, followed by UV irradiation. As shown in Figure 7d, CSIG overexpression increased Bax expression. Overexpression of p33ING1 increased CSIG level and the

target gene Bax expression to an extent that was comparable with cotransfection with CSIG. Knocking down CSIG protein significantly reduced activation of Bax by p33ING1 introduction, suggesting that CSIG is essential for p33ING1 signaling. Moreover, CSIG and p33ING1 overexpression did not change HSP70 and PTEN expressions. Similar results have been obtained using HeLa cells (Supplementary Figure S4b). To further determine the effect of knocking down CSIG on Bax-dependent apoptosis in mitochondria induced by p33ING1, we examined the mitochondrial distribution of Bax and release of cytochrome *c* to the cytoplasm after UV. As shown in Figure 7e, knocking down CSIG decreased induction of mitochondrial Bax expression and translocation of cytochrome *c* to the cytoplasm by p33 introduction.

Consistent with these results, overexpression of p33ING1 and CSIG enhanced UV-induced apoptosis, as determined by cleaved caspase 3, cleaved PARP, and Annexin-V and PI double staining. Apoptosis analysis by cotransfection of p33ING1 and CSIG was comparable to transfection with p33ING1 or CSIG alone, while knocking down CSIG protein abrogated the effect of p33ING1 (Figures 7d and f). Overexpression of p33ING1 did not increase CSIG protein stability and apoptosis markedly without UV treatment (Supplementary Figure S5). Taken together, these results demonstrate that p33ING1–CSIG functions in UV-induced apoptosis and CSIG is required for p33ING1 signaling after UV irradiation.

**The p33ING1–CSIG axis functions in differential apoptotic responses of the young and old 2BS cells after UV irradiation.** We previously showed that in human diploid 2BS fibroblasts, senescent fibroblasts are more resistant than young fibroblasts to apoptosis.<sup>30,31</sup> Here, we showed that young 2BS cells were more sensitive than senescent cells to UV-induced apoptosis, as shown

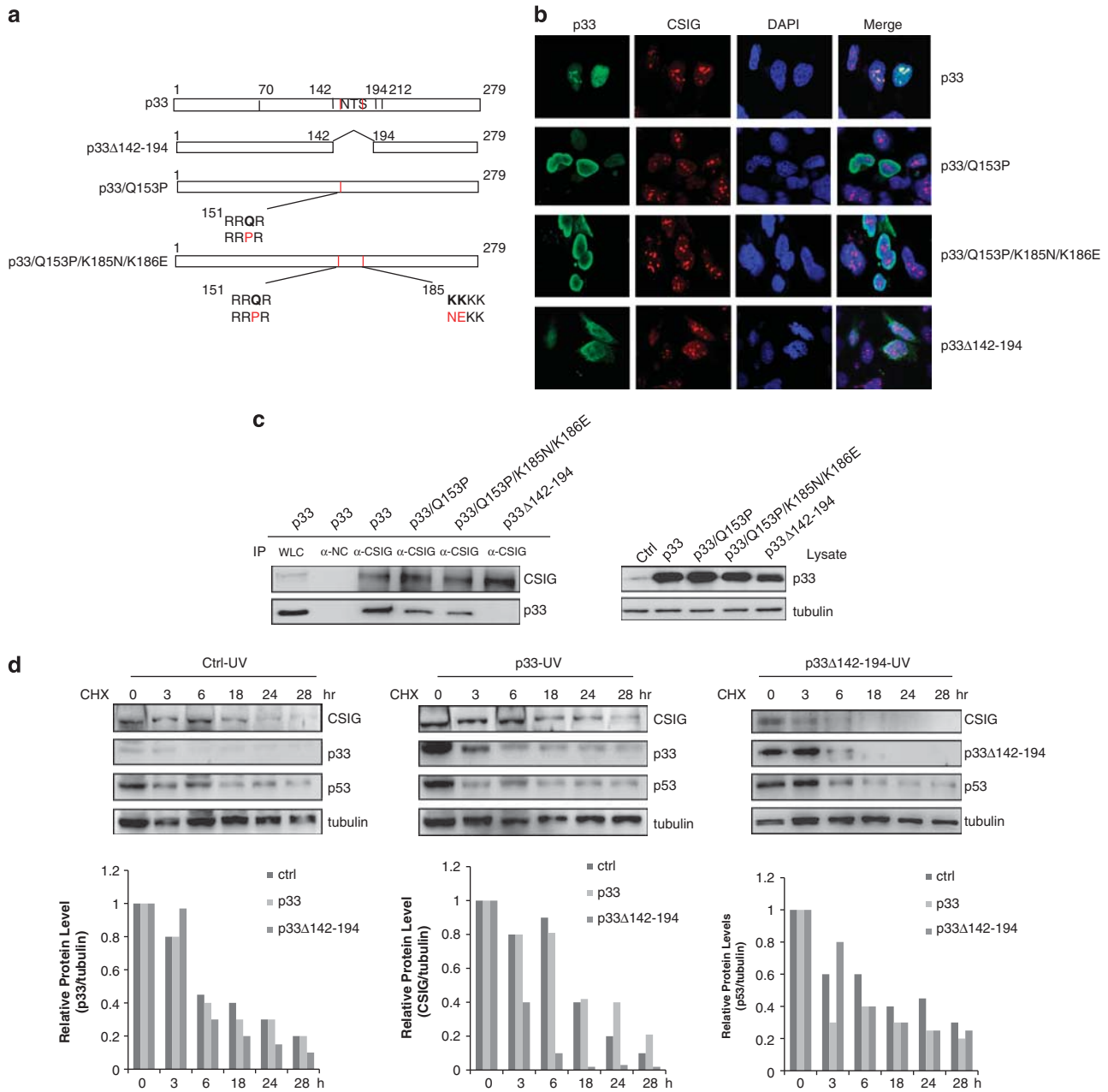


**Figure 6** p33ING1 requires its NTS region to bind to and stabilize CSIG protein. (a) Schematic representation of p33 and its mutants in NTS region. Deletion or point mutations of NTS are shown. (b) Cells were transfected with expression vectors encoding wild-type p33, p33/Q153P, p33/Q153P/K185N/K186E and p33Δ142–194. After 36 h, cells were stained with anti-p33 antibody (green) and anti-CSIG antibody (red) analyzed by confocal microscopy. Nuclei are shown in blue (DAPI staining). (c) HEK293 cells were transfected with wild-type p33, p33/Q153P, p33/Q153P/K185N/K186E and p33Δ142–194 plasmids. IP experiments were performed with anti-CSIG antibody or non-related serum (NC). Western blot analysis was performed with indicated antibodies. Cell lysates were loaded as control. (d) Control vector, vectors expressing p33 or p33Δ142–194 were transfected in HEK293 cells as indicated. At 36 h after transfection, cells were subjected to UV irradiation and treated with cycloheximide (CHX, 100 μg/ml) for the indicated times. CSIG protein levels were analyzed by western blotting. p53 levels were determined as positive control. The densitometry analysis of p33, CSIG and p53 protein of different groups were listed below

by cleavage of PARP (Figure 8a). Based on the above results, we hypothesized that the p33ING1–CSIG axis has a role in differential apoptotic responses of 2BS cells during replicative senescence. To study this possibility, expressions of CSIG and p33ING1 in early passage (young, ~20 population doublings (pdl)) and late-passage (senescent, ~60 pdl) 2BS cells were examined by western blot. As shown in Figure 8b, compared with early passage 2BS cells

(young, Y), we found CSIG and p33ING1 levels in late-passage 2BS cells (senescent, S) were significantly reduced. Expression of p16<sup>INK4a</sup> is an indication of 2BS cells undergoing replicative senescence. We then analyzed the expression and cellular localization of CSIG and p33ING1 in young and senescent 2BS cells after UV irradiation. As shown in Figure 8c, CSIG and p33ING1 protein increased within 6 h and remained at relatively high levels after UV

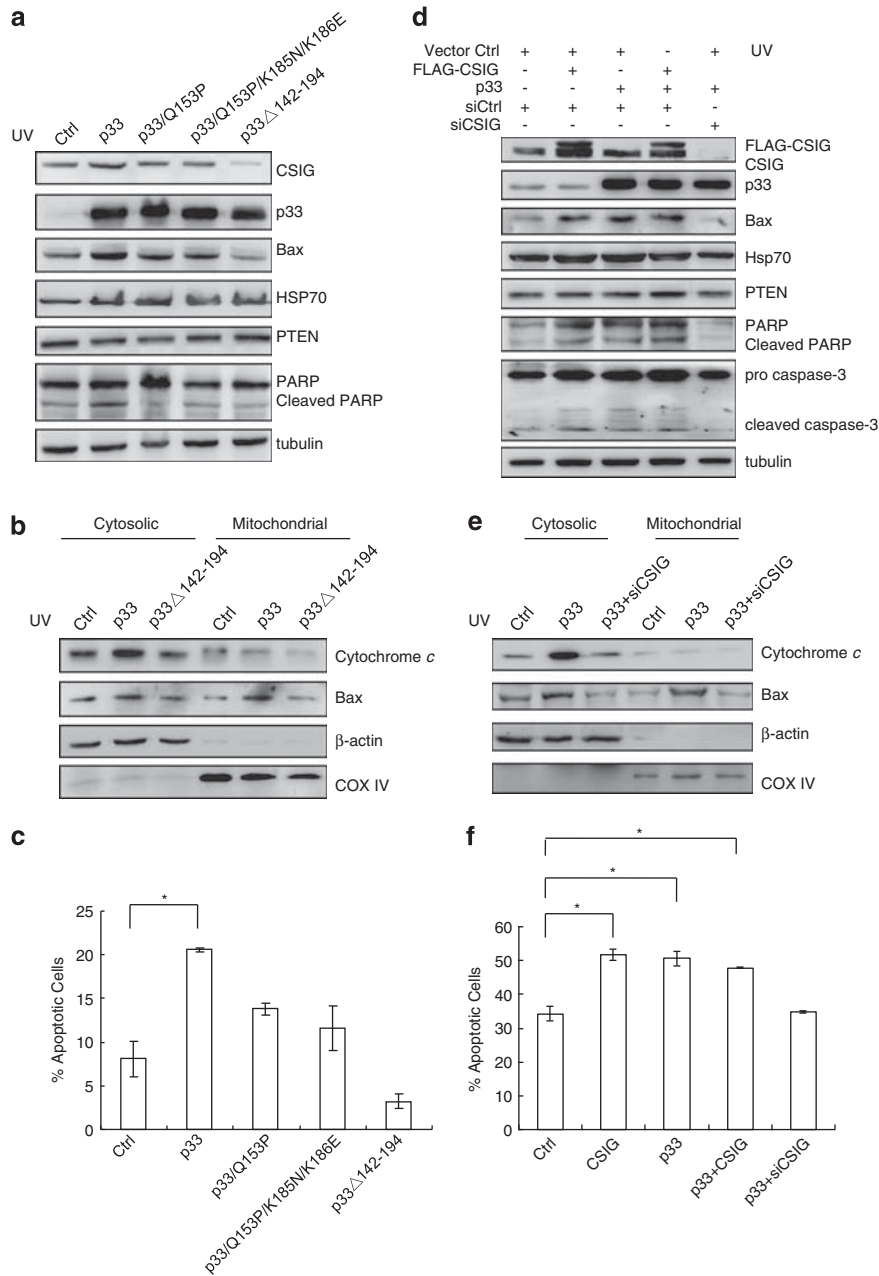


**Figure 7** p33ING1 requires CSIG protein to activate target gene expression and promote UV-induced apoptosis. **(a)** HEK293 cells were transfected with control vector or a vector expressing wild-type p33, p33/Q153P, p33/Q153P/K185N/K186E or p33Δ142–194. At 36 h after transfection, cells were subjected to UV irradiation, and 12 h after UV treatment, western blot were performed to detect changes in CSIG and target proteins of p33 and CSIG. **(b)** HEK293 cells were transfected with control vector, wild-type p33 and p33Δ142–194; cells were then subjected to UV treatment. Protein extracts were divided into cytosol and mitochondrial fractions and analyzed by western blotting with antibodies against cytochrome *c* and Bax. Fractionation quality was verified by specific subcellular markers ( $\beta$ -actin as a cytoplasm-specific marker and COX IV protein as mitochondria-specific marker). **(c)** HEK293 cells were transfected with control vector or a vector expressing wild-type p33, p33/Q153P, p33/Q153P/K185N/K186E or p33Δ142–194. At 36 h after transfection, cells were subjected to UV irradiation. After 12 h, apoptosis was analyzed by Annexin V–FITC and PI double staining followed by FACS. **(d)** Vectors expressing p33, CSIG and siRNAs against CSIG were transfected alone or in combination into HEK293 cells. At 36 h after transfection, cells were subjected to UV irradiation, and 24 h after UV treatment, western blot were performed to detect changes in target proteins of p33 and CSIG by indicated antibodies. **(e)** Vector expressing p33 was transfected alone or in combination with siRNAs against CSIG into HEK293. Cells were then subjected to UV treatment. Protein extracts were divided into cytosol and mitochondrial fractions and analyzed by western blotting with antibodies against cytochrome *c* and Bax. Fractionation quality was verified by specific subcellular markers  $\beta$ -actin and COX IV protein. **(f)** Apoptosis was analyzed by Annexin V–FITC and PI double staining followed by FACS. The percentage of apoptotic cells was quantitated. Values are means  $\pm$  S.D. from independent experiments. \* $P \leq 0.05$

irradiation in young 2BS cells, while in senescent 2BS cells, CSIG and p33ING1 levels decreased after UV. Using immunocytochemistry, we found that after UV irradiation, p33ING1 colocalized extensively with CSIG to the nucleolus

in young 2BS cells; however, in senescent 2BS cells, the expression levels and the nucleolar colocalization of p33ING1 and CSIG decreased (Figure 8d). p33ING1 facilitated UV-induced apoptosis, while knockdown CSIG



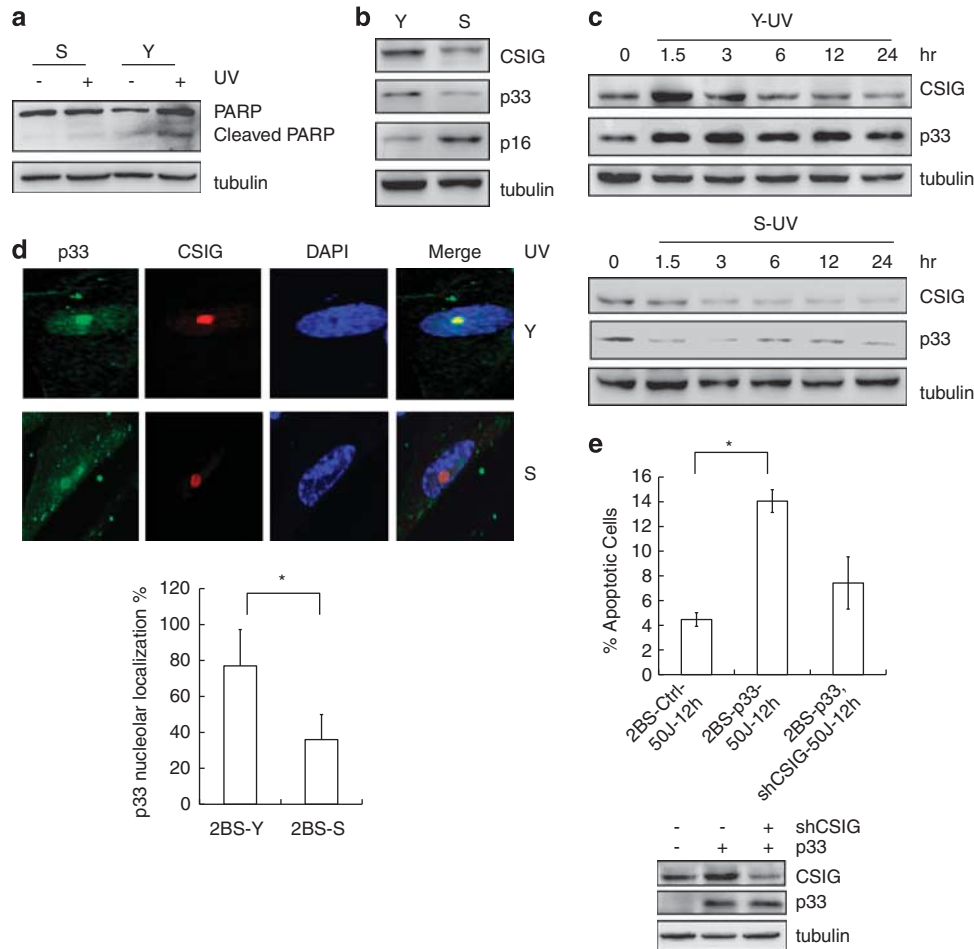


**Figure 8** Expressions and colocalization of CSIG and p33ING1 in young and senescent human diploid 2BS fibroblasts after UV irradiation. (a) Young and senescent 2BS cells were treated with 50 J/m<sup>2</sup> UV or mock treated, and expression of full-length and cleaved PARP were detected by western blot analysis. (b) Western blot analysis of CSIG and p33 levels in early passage (young, ~20 pdl, Y) and late-passage (senescent, ~60 pdl, S) 2BS cells. p16 served as an indicator of cellular senescence and  $\alpha$ -tubulin served as loading control. (c) Young and senescent 2BS cells were irradiated with 50 J/m<sup>2</sup> UV and cells were collected at different time points as indicated. Immunoblot analysis was carried out using anti-CSIG, anti-p33 and anti-tubulin antibodies. (d) Young and senescent 2BS cells were irradiated with 50 J/m<sup>2</sup> UV 24 h after UV irradiation; cells were immunostained with anti-p33 and anti-CSIG antibodies, followed by confocal microscopy analysis. Representative images are shown. Nuclei were visualized by DAPI staining and images were overlaid (Merge). Quantitative analysis of the nucleolar distribution of p33ING1 was by counting three fields (at least 100 cells per field). (e) 2BS cells were infected with p33 alone or in combination of shCSIG, cells then were treated with 50 J/m<sup>2</sup> UV, 12 h later, apoptotic cell numbers were detected. Values are means  $\pm$  S.D. from independent experiments. \* $P \leq 0.05$

expression reversed the effects of p33ING1 in 2BS cells (Figure 8e). These results suggest the p33ING1–CSIG axis may have a role in differential apoptotic responses of the young and old 2BS cells after UV irradiation.

## Discussion

There is now a compelling body of evidence showing that, in addition to ribogenesis pathway, nucleolar proteins have important roles in regulating cell-cycle transition, cell proliferation and apoptosis.<sup>4,5</sup> We set out to determine if nucleolar protein CSIG is involved in DNA damage-induced apoptosis, and found, for the first time, that CSIG is induced after UV irradiation and overexpression of CSIG increases apoptotic cells. Although CSIG does not induce apoptosis in the absence of DNA damage, it promotes apoptosis after UV irradiation (Figure 1). Ultraviolet irradiation produces DNA lesions that perturb DNA metabolism, activating some

proteins that regulate cell-cycle arrest or apoptosis. High-level damage can overwhelm the ability of the repair mechanism to remove lesion such as 6–4PPs, and it may lead to cell-cycle arrest at the G<sub>2</sub>/M phase, which often precedes the onset of apoptosis. Inability to repair replication-induced damage over time triggers apoptosis. We showed here that CSIG could slightly decrease G<sub>1</sub>-phase cells, and increase S-phase and G<sub>2</sub>/M-phase cells, after UV irradiation; however, there was no significant difference compared with control. These results suggest that CSIG's function after UV irradiation relates to apoptosis rather than cell-cycle control.

The most common isoform of ING1 is p33ING1; agents that damage DNA could increase p33ING1 expression in certain cell lines.<sup>20,24</sup> Although p33ING1 and p53 have a functional relevance in certain biological process,<sup>22</sup> there are studies showing p33ING1 could exert a p53-independent function in apoptosis or cell growth inhibition.<sup>23,32</sup> A previous investigation reported that UV stress could translocate the p33ING1

protein from the nucleoplasm to the nucleolus though two distinct four amino-acid sequences in NTS region; this translocation of p33ING1 is essential for UV-induced apoptosis.<sup>12</sup> However, the mechanism by which the nucleolar targeting of p33ING1 promotes apoptosis is not clear.

We found that the proteins p33ING1 and CSIG are highly colocalized in the nucleolus after UV stress, and p33ING1 expression induction corresponds with nucleolar protein CSIG after UV irradiation (Figure 2). More importantly, the NTS region of p33ING1 is required to bind and increase CSIG protein stability, which in turn is essential for p33-mediated apoptosis (Figures 3–7). We show here that CSIG is necessary for the p33ING1 pro-apoptosis function. Expression of the p33ING1 downstream target gene, *Bax*, is controlled by CSIG in UV-induced apoptosis (Figure 7).

After DNA damage, some nucleolar proteins can regulate p53-dependent apoptosis through inhibition of Mdm2, enhancing p53 translation and enhancing p53 translocation to mitochondria.<sup>33,34</sup> Therefore, a possible mechanism of regulatory *Bax* expression by CSIG could be activation of p53 leading to *Bax* activation after UV treatment. Some other nucleolar proteins have pro-apoptotic functions involving regulation of *Bax*, *Bcl-2*, caspase activity or cell surface receptors.<sup>33,34</sup> A subset of nucleolar proteins can directly control gene transcription or functionally modulate transcriptional regulators.<sup>34</sup> Reportedly, CSIG upregulates the *uPA* (urokinase-type plasminogen activator) gene transcription.<sup>35</sup> The p33ING1 protein is a stoichiometric component of HAT and HDAC complexes, and p33ING1 can regulate gene transcription through recognition of H3K4me3.<sup>36,37</sup> Therefore, it is also possible that CSIG may by itself or cooperate with p33ING1 to regulate target gene expression, and after UV irradiation, the regulatory functions of CSIG or p33ING1–CSIG on downstream targets may be enhanced. There are several possible regulatory mechanisms of this process and further studies will be required to elucidate the possibilities.

The above observations led us to propose a model for the pro-apoptotic function of p33ING1–CSIG axis after UV irradiation. This model is also supported by our findings in human diploid 2BS fibroblasts, in which p33ING1–CSIG axis may function in differential apoptotic responses of the young and senescent 2BS cells after UV treatment (Figure 8). In summary, our study establishes a novel pro-apoptosis function of CSIG and its relationship with p33ING1 after UV irradiation.

## Materials and Methods

**Antibodies and chemicals.** Antibodies for p53 (anti-p53 PAb421, DO-1 and mouse monoclonal antibody), p27, ARF, HDAC1, HDAC2, PTEN, HSP70, *Bax*, caspase-3, cytochrome *c*, cytochrome *c* oxidase IV (COX IV) and  $\beta$ -actin were purchased from Santa Cruz Biotechnology (Santa Cruz, CA, USA). Anti-CSIG was used as previously described<sup>13</sup> or purchased from Abcam (Cambridge, MA, USA). Anti-p33ING1 antibodies were from Abcam, Millipore (Billerica, MA, USA) or Santa Cruz Biotechnology; the antibody from Abcam detects p33ING1 but does not cross react with p24ING1 or p47ING1, and the antibodies from Millipore and Santa Cruz Biotechnology recognize all the three isoforms. Anti-FLAG was obtained from Sigma (St. Louis, MO, USA). Anti- $\alpha$ -tubulin and anti-p16<sup>INK4a</sup> were obtained from Millipore. Anti-PARP was obtained from Cell Signaling Technology (Danvers, MA, USA) and anti-GST was obtained from Abgent (San Diego, CA, USA). Anti-multi-ubiquitin was obtained from MBL (Woburn, MA, USA). Cisplatin, etoposide, doxorubicin, cycloheximide, MG-132 and DAPI and G418 are all obtained from Sigma.

**Plasmids and siRNA preparations.** The full-length p33ING1 cDNA was kindly provided by Dr Karl Riabowol. The full-length CSIG cDNA was described previously.<sup>13</sup> FLAG-p33ING1, FLAG-p33-NT, FLAG-p33-CT and p33 $\Delta$ 142–194 were amplified from p33ING1 by PCR using FLAG-tagged primers at the N-terminus, and inserted between EcoRI and BamHI sites in pIRES neo2 vector (Clontech, Mountain View, CA, USA). ER:p33ING1 was amplified from p33ING1 by PCR, and inserted into NotI and Sall sites of xER-LNCX2 vector. FLAG-CSIG, FLAG-CSIG-NT and FLAG-CSIG-CT were amplified from CSIG by PCR, and inserted into pIRES neo2 with N-terminus FLAG tags. p33/Q153P and p33/Q153P/K185N/K186E were generated using the QuikChange Site-Directed Mutagenesis kit (Stratagene, Santa Clara, CA, USA). GST–CSIG was constructed by cloning full-length CSIG in pGEX-4T-1 vector (GE Healthcare, Piscataway, NJ, USA). The siRNA was designed as reported previously. siRNA targeting CSIG was 5'-AGAAGGAACAGACGCCAGA-3' and negative control siRNA was 5'-AAGTGTAGTAGATCACCAGC-3'.<sup>13</sup> siRNA targeting p33ING1 was 5'-ACCCACGTACTGTCTGTGCAA-3'.<sup>38</sup>

**Cell culture and transfection.** Human diploid 2BS fibroblasts (National Institute of Biological Products, Beijing, China), HEK293, HeLa, the wild-type p53 and p53-null HCT116, RKO, RKO-E6 and H1299 cells were cultured in Dulbecco's modified Eagle's medium (Invitrogen, Grand Island, NY, USA) supplemented with 10% fetal bovine serum at 37°C in 5% CO<sub>2</sub>.

Cells were plated on 60-mm or 100-mm culture dishes. For UV irradiation, culture medium was removed and culture dishes were uncovered in a UV cross-linker (model UVC-500; Hoefer, Holliston, MA, USA). Cells were irradiated at the range from 25 to 200 J/m<sup>2</sup> UVC in initial dose response assays, and 50 J/m<sup>2</sup> was finally employed. Immediately after irradiation, medium was added back, and cells were cultured for appropriate time.

All plasmids were transfected using Lipofectamine 2000 (Invitrogen) and siRNA were transfected using RNAiMAX (Invitrogen) following the manufacturer's instructions. Stable cell lines were obtained by sustained selection with G418.

**Western blotting, IP and GST pull-down assay.** Following treatment, all the floating and adherent cells were collected. Whole-cell extracts, nuclear extracts or cytoplasmic extracts were prepared, and western blots were done as previously described.<sup>13</sup> For mitochondrial and cytosolic extracts preparation, cells were lysed in buffer (250 mM sucrose, 20 mM HEPES, 10 mM KCl, 1.5 mM MgCl<sub>2</sub>, 1 mM EDTA, 1 mM EGTA, 1 mM dithiothreitol, 1 mM PMSF, 10  $\mu$ g/ml aprotinin and 10  $\mu$ g/ml leupeptin at pH 7.5) and incubated for 30 min on ice. Cells were homogenized by 30 strokes in a 22-gauge needle. Homogenates were centrifuged at 750 *g* for 10 min at 4°C. Supernatants were centrifuged at 10 000 *g* for 15 min at 4°C to collect the mitochondrial pellets.

For IP, cells were collected from a 10-cm-diameter plate using RIPA buffer containing protease inhibitor cocktail (Roche, Basel, Switzerland). Lysates were precleared by incubation with 100  $\mu$ l of protein A-Sepharose (50% slurry) for 1 h. The cleared lysate was then subjected to IP with the indicated antibodies overnight at 4°C. Protein A-Sepharose beads (GE Healthcare) were added and the incubation was continued for 2 h at 4°C. Precipitates were washed four times with RIPA buffer (1 ml), followed by resuspension in 2  $\times$  SDS loading buffer. Proteins were separated using gradient SDS-PAGE gels; western blotting was carried out according to standard procedures.

Recombinant GST or GST–CSIG fusion proteins were expressed in and purified from BL21 cells as described. *In vitro*-translated p33ING1 protein was generated using the TNT-coupled Transcription/Translation system (Promega, Madison, WI, USA). Wild-type p33ING1 were incubated with GST or GST–CSIG bacterial recombinant protein immobilized on glutathione–Sepharose 4B resin at 4°C for 2 h. Beads were then washed five times in 1 ml wash buffer (20 mM Tris/HCl pH 8.0, 0.5 mM EDTA, 10% (v/v) glycerol, 0.5% (v/v) NP-40 and 200 mM KCl). The bound proteins were eluted with 2  $\times$  SDS sample buffer, fractionated by SDS-PAGE and subjected to western blot analysis with anti-p33 antibody.

**Immunofluorescence.** Cells were seeded on coverslips; they were transfected with indicated plasmids, left untreated or exposed to ultraviolet irradiation. Cells were fixed with 4% paraformaldehyde in phosphate-buffered saline (PBS) for 10 min, permeabilized with 0.5% Triton X-100 in PBS for 10 min and incubated in blocking solution (PBS containing 2% bovine serum albumin) for 2 h at room temperature. Coverslips were incubated for 1 h in a 1 : 400 dilution of mouse anti-p33ING1 and rabbit anti-CSIG prepared in blocking buffer. Cells were washed with PBS (3–4 washes, 15 min each) before incubation with a mixture of Alexa 488 goat anti-mouse (1 : 400; Invitrogen) and Alexa 647 donkey anti-rabbit (1 : 400; Invitrogen) secondary antibodies. After washing in the same conditions using the

primary antibodies, chromosomal DNA was examined by staining with DAPI. Stained cells were mounted on glass slides and examined with a confocal laser microscope (Leica, Buffalo Grove, IL, USA). Representative photographs from three independent experiments are shown.

**Apoptosis assays.** Apoptosis was evaluated by morphological examination using DAPI staining. Annexin V-FITC double staining assay was performed according to the manufacturer's protocol (Calbiochem, San Diego, CA, USA). Cells were transfected with indicated vectors for 24 h, then irradiated by UV and recovered for indicated times. Cells were harvested and centrifuged at 1500 r.p.m. for 5 min at room temperature. Medium was removed and cells were washed once in PBS. Cells were then resuspended in cold binding buffer and both Annexin V-FITC and PI were added. Samples were then incubated at room temperature for 15 min in the dark and analyzed by flow cytometry. Cells were also fixed in 70% ethanol and incubated in PBS containing 50  $\mu$ g/ml RNase and 2.5  $\mu$ g/mL propidium iodide. DNA content was analyzed by flow cytometry. The percentage of cells with sub-G1 DNA was determined with the ModFit LT Program (Verity Software, Verity Software House, Topsham, ME, USA).

**Statistical analysis.** The data are reported as mean  $\pm$  S.D. of the indicated number of experiments. Values were assessed by pairwise one-way analysis of variance (ANOVA). In all cases,  $*P \leq 0.05$  was considered significant.

### Conflict of Interest

The authors declare no conflict of interest.

**Acknowledgements.** We are sincerely grateful to Professor Karl Riabowol, who generously provided the p33ING1 plasmid. We thank Drs Wengong Wang and Jun Chen for helpful discussions. This work was supported by grants from the National Basic Research Programs of China, No.2012CB911200 and the National Natural Science Foundation of China, No.81170319 and No. 31071206.

- Andersen JS, Lyon CE, Fox AH, Leung A, Lam YW, Steen H *et al*. Directed proteomic analysis of the human nucleolus. *Curr Biol* 2002; **12**: 1.
- Pederson T. The plurifunctional nucleolus. *Nucleic Acids Res* 1998; **26**: 3871–3876.
- Boulton S, Westman BJ, Hutten S, Boisvert F, Lamond AI. The nucleolus under stress. *Mol Cell* 2010; **40**: 216–227.
- Pederson T, Tsai R. In search of nonribosomal nucleolar protein function and regulation. *J Cell Biol* 2009; **184**: 771–776.
- Ma LW, Chang N, Guo SZ, Li Q, Zhang ZY, Wang WG *et al*. CSIG inhibits PTEN translation in replicative senescence. *Mol Cell Biol* 2008; **28**: 6290–6301.
- Meng LJ, Yasumoto H, Tsai R. Multiple controls regulate nucleostemin partitioning between nucleolus and nucleoplasm. *J Cell Sci* 2006; **119**: 5124–5136.
- Andersen JS, Lam YW, Leung A, Ong SE, Lyon CE, Lamond AI *et al*. Nucleolar proteome dynamics. *Nature* 2005; **433**: 77–83.
- Tembe V, Henderson BR. Protein trafficking in response to DNA damage. *Cell Signal* 2007; **19**: 1113–1120.
- Bernardi R, Scaglioni PP, Bergmann S, Horn HF, Vousden KH, Pandolfi PP. PML regulates p53 stability by sequestering Mdm2 to the nucleolus. *Nat Cell Biol* 2004; **6**: 665–672.
- Kotoglou P, Kalaitzakis A, Vezyraki P, Tzavaras T, Michalis LK, Dantzer F *et al*. Hsp70 translocates to the nuclei and nucleoli, binds to XRCC1 and PARP-1, and protects HeLa cells from single-strand DNA breaks. *Cell Stress Chaperon* 2009; **14**: 391–406.
- Loveridge CJ, MacDonald A, Thoms HC, Dunlop MG, Stark LA. The proapoptotic effects of sulindac, sulindac sulfone and indomethacin are mediated by nucleolar translocation of the RelA(p65) subunit of NF- $\kappa$ B. *Oncogene* 2008; **27**: 2648–2655.
- Scott M, Boisvert FM, Vieyra D, Johnston RN, Bazett-Jones DP, Riabowol K. UV induces nucleolar translocation of ING1 through two distinct nucleolar targeting sequences. *Nucleic Acids Res* 2001; **29**: 2052–2058.
- Stegh AH, Schickling O, Ehret A, Scaffidi C, Peterhansel C, Hofmann TG *et al*. DEDD, a novel death effector domain-containing protein, targeted to the nucleolus. *EMBO J* 1998; **17**: 5974–5986.
- Garkavtsev I, Kazarov A, Gudkov A, Riabowol K. Suppression of the novel growth inhibitor p33(ING1) promotes neoplastic transformation. *Nat Genet* 1996; **14**: 415–420.
- Cheung KJ, Li G. P33(ING1) enhances UVB-induced apoptosis in melanoma cells. *Exp Cell Res* 2002; **279**: 291–298.

- Helbing CC, Veillette C, Riabowol K, Johnston RN, Garkavtsev I. A novel candidate tumor suppressor, ING1, is involved in the regulation of apoptosis. *Cancer Res* 1997; **57**: 1255–1258.
- Gonzalez L, Freije J, Cal S, Lopez-Otin C, Serrano M, Palmero I. A functional link between the tumour suppressors ARF and p33ING1. *Oncogene* 2006; **25**: 5173–5179.
- Lee C, Smith BA, Bandyopadhyay K, Gjerset RA. DNA damage disrupts the p14ARF-B23(nucleophosmin) interaction and triggers a transient subnuclear redistribution of p14ARF. *Cancer Res* 2005; **65**: 9834–9842.
- Yogev O, Saadon K, Anzi S, Inoue K, Shauhan E. DNA damage-dependent translocation of B23 and p19(ARF) is regulated by the Jun N-terminal kinase pathway. *Cancer Res* 2008; **68**: 1398–1406.
- Cheung K, Bush JA, Jia W, Li G. Expression of the novel tumour suppressor p33(ING1) is independent of p53. *Brit J Cancer* 2000; **83**: 1468–1472.
- Shimada H, Liu TL, Ochiai T, Shimizu T, Haupt Y, Hamada H *et al*. Facilitation of adenoviral wild-type p53-induced apoptotic cell death by overexpression of p33(ING1) in T.Tn human esophageal carcinoma cells. *Oncogene* 2002; **21**: 1208–1216.
- Shinoura N, Muramatsu Y, Nishimura M, Yoshida Y, Saito A, Yokoyama T *et al*. Adenovirus-mediated transfer of p33(ING1) with p53 drastically augments apoptosis in gliomas. *Cancer Res* 1999; **59**: 5521–5528.
- Tsang FC, Po LS, Leung KM, Lau A, Siu WY, Poon R. ING1b decreases cell proliferation through p53-dependent and -independent mechanisms. *FEBS Lett* 2003; **553**: 277–285.
- Garate M, Campos EI, Bush JA, Xiao H, Li G. Phosphorylation of the tumor suppressor p33(ING1b) at Ser-126 influences its protein stability and proliferation of melanoma cells. *FASEB J* 2007; **21**: 3705–3716.
- Abad M, Menendez C, Fuchtbauer A, Serrano M, Fuchtbauer EM, Palmero I. Ing1 mediates p53 accumulation and chromatin modification in response to oncogenic stress. *J Biol Chem* 2007; **282**: 31060–31067.
- Garkavtsev I, Grigorian IA, Ossovskaya VS, Chernov MV, Chumakov PM, Gudkov AV. The candidate tumour suppressor p33(ING1) cooperates with p53 in cell growth control. *Nature* 1998; **391**: 295–298.
- Leung KM, Po LS, Tsang FC, Sin WY, Lau A, Ho H *et al*. The candidate tumor suppressor ING1b can stabilize p53 by disrupting the regulation of p53 by MDM2. *Cancer Res* 2002; **62**: 4890–4893.
- Feng XL, Bonni S, Riabowol K. HSP70 induction by ING proteins sensitizes cells to tumor necrosis factor alpha receptor-mediated apoptosis. *Mol Cell Biol* 2006; **26**: 9244–9255.
- Nagashima M, Shiseki M, Miura K, Hagiwara K, Linke SP, Pedoux R *et al*. DNA damage-inducible gene p33ING2 negatively regulates cell proliferation through acetylation of p53. *P Natl Acad Sci USA* 2001; **98**: 9671–9676.
- Huang Y, Corbly MJ, Tang ZQ, Yang L, Peng Y, Zhang ZY *et al*. Down-regulation of p21(WAF1) promotes apoptosis in senescent human fibroblasts: involvement of retinoblastoma protein phosphorylation and delay of cellular aging. *J Cell Physiol* 2004; **201**: 483–491.
- Huang Y, Yang L, Zhang ZY, Tong TJ. Exogenous p21(WAF1) transfection affects apoptosis in human fibroblasts. *Acta Biochimica ET Biophysica Sinica* 2000; **32**: 35–38.
- Coles AH, Liang HL, Zhu ZQ, Marfella C, Kang J, Imbalzano AN *et al*. Deletion of p37(Ing1) in mice reveals a p53-independent role for Ing1 in the suppression of cell proliferation, apoptosis, and tumorigenesis. *Cancer Res* 2007; **67**: 2054–2061.
- Kerr LE, Birse-Archbold J, Short DM, McGregor AL, Heron I, MacDonald DC *et al*. Nucleophosmin is a novel Bax chaperone that regulates apoptotic cell death. *Oncogene* 2007; **26**: 2554–2562.
- Lindstrom MS. Emerging functions of ribosomal proteins in gene-specific transcription and translation. *Biochem Bioph Res Co* 2009; **379**: 167–170.
- Tong C, Tan L, Li P, Zhu YS. Identification of a novel nucleus protein involved in the regulation of urokinase in 95D cells. *Acta Biochimica ET Biophysica Sinica* 2005; **37**: 303–309.
- Feng XL, Hara Y, Riabowol KT. Different HATS of the ING1 gene family. *Trends Cell Biol* 2002; **12**: 532–538.
- Pena PV, Hom RA, Hung T, Lin H, Kuo AJ, Wong R *et al*. Histone H3K4me3 binding is required for the DNA repair and apoptotic activities of ING1 tumor suppressor. *J Mol Biol* 2008; **380**: 303–312.
- Kuo W, Wang YM, Wong R, Campos EI, Li G. The ING1b tumor suppressor facilitates nucleotide excision repair by promoting chromatin accessibility to XPA. *Exp Cell Res* 2007; **313**: 1628–1638.



**Cell Death and Disease is an open-access journal published by Nature Publishing Group. This work is licensed under the Creative Commons Attribution-NonCommercial-No Derivative Works 3.0 Unported License. To view a copy of this license, visit <http://creativecommons.org/licenses/by-nc-nd/3.0/>**

Supplementary Information accompanies the paper on Cell Death and Disease website (<http://www.nature.com/cddis>)